Current global plate kinematics from GPS (1995–2007) with the plate-consistent reference frame

Mikhail G. Kogan[1] and Grigory M. Steblov[1,2]

Received 28 August 2007; revised 29 December 2007; accepted 21 January 2008; published 30 April 2008.

[1] We present the vectors of rotation of 10 major lithospheric plates, estimated from continuous GPS observations at 192 globally distributed stations; 71 stations were selected as representing stable plate regions. All days for the period 1995.0–2007.0 were included in the analysis. In contrast to previous GPS plate models, our model is independent of international terrestrial reference frames (ITRF). The origin of our plate-consistent reference frame is the center of plate rotation (CP) rather than the center of mass of the entire Earth's system (CM) as in recent versions of ITRF. We estimate plate rotations and CP by minimizing the misfit between the horizontal velocities predicted by the plate model and the observed GPS velocities. If any version of ITRF is used as the reference frame, the drift of the ITRF origin relative to CP cannot be neglected in estimation of plate rotation vectors and plate-residual station velocities. The model of the plate kinematics presented here addresses the problem debated since the beginning of the space geodesy: how big are disagreements between the current plate motions and the motions averaged over several million years? We compare the vectors of relative plate rotations estimated here with the published vectors from GPS and geologic models. We also discuss the integrity of individual plates as exhibited by plate-residual station velocities. For seven largest plates, the RMS value of plate-residual station velocities in stable plate interiors is 0.5–0.9 mm/a; this value is an upper bound on deviation of real plates from infinite stiffness.

Citation: Kogan, M. G., and G. M. Steblov (2008), Current global plate kinematics from GPS (1995–2007) with the plate-consistent reference frame, *J. Geophys. Res.*, *113*, B04416, doi:10.1029/2007JB005353.

1. Introduction

[2] This paper presents a model of motion of 10 major lithospheric plates, estimated from continuous GPS observations at 192 globally distributed stations for the period 1995.0–2007.0; 71 stations were selected as representing stable plate regions (Figure 1). We included in the analysis all daily global solutions of the Scripps Orbital and Permanent Array Center (SOPAC) for positions of the International Global Navigation Satellite System (GNSS) Service (IGS) network; SOPAC solutions were combined with our solutions for a number of additional stations essential for the plate tectonic analysis. In contrast to published models, we included longer time series since the start of the International GPS Service (1994), with observations extended to a more recent epoch.

[3] There are several definitions of the Earth's center (see details in the work by *Argus et al.* [1999], *Blewitt* [2003], *Dong et al.* [2003], and *Argus* [2007]): CM, the center of mass of the Earth, oceans, and atmosphere; CE, the center of mass of the solid Earth; CF, the center of the Earth's surface figure, that is, the mean position of an ideal, uniform, dense set of stations on the Earth's surface; and CL, the center of the Earth's lateral figure chosen so that the integral of the horizontal displacement over the Earth's surface is zero.

[4] Published GPS models of the global plate kinematics were estimated in reference frames of the ITRF series, mostly ITRF97 or ITRF2000 [*Argus and Heflin*, 1995; *Larson et al.*, 1997; *Sella et al.*, 2002; *Kreemer et al.*, 2003; *Prawirodirdjo and Bock*, 2004]. The origin of ITRF97 was placed at CF by the Helmert transformation of VLBI, SLR, and GPS solutions to best fit the velocities predicted by the geologic plate model NUVEL-1A. This definition suffers from errors in NUVEL-1A [*DeMets and Dixon*, 1999; *Calais et al.*, 2003b; *Steblov et al.*, 2003]. The origins of ITRF2000 and ITRF2005 are placed at CM as sampled by SLR observations [*Altamimi et al.*, 2002]. The origin of ITRF2005 moves relative to ITRF2000 at a speed of ~2 mm/a. Such poor agreement between both ITRF versions arises from uncertainties in SLR station velocities [*Altamimi et al.*, 2007; *Argus*, 2007].

[5] In this study, we use the plate-consistent reference frame with the origin at the center of plate rotation (CP), that is, the center of the sphere comprising lithospheric plates. Our initial loosely constrained GPS solution for velocities is referenced to the coordinate system whose

[1] Lamont-Doherty Earth Observatory of Columbia University, Palisades, New York, USA.
[2] Also at Institute of Physics of the Earth, Russian Academy of Sciences, Moscow, Russia.

0148-0227/08/2007JB005353$09.00

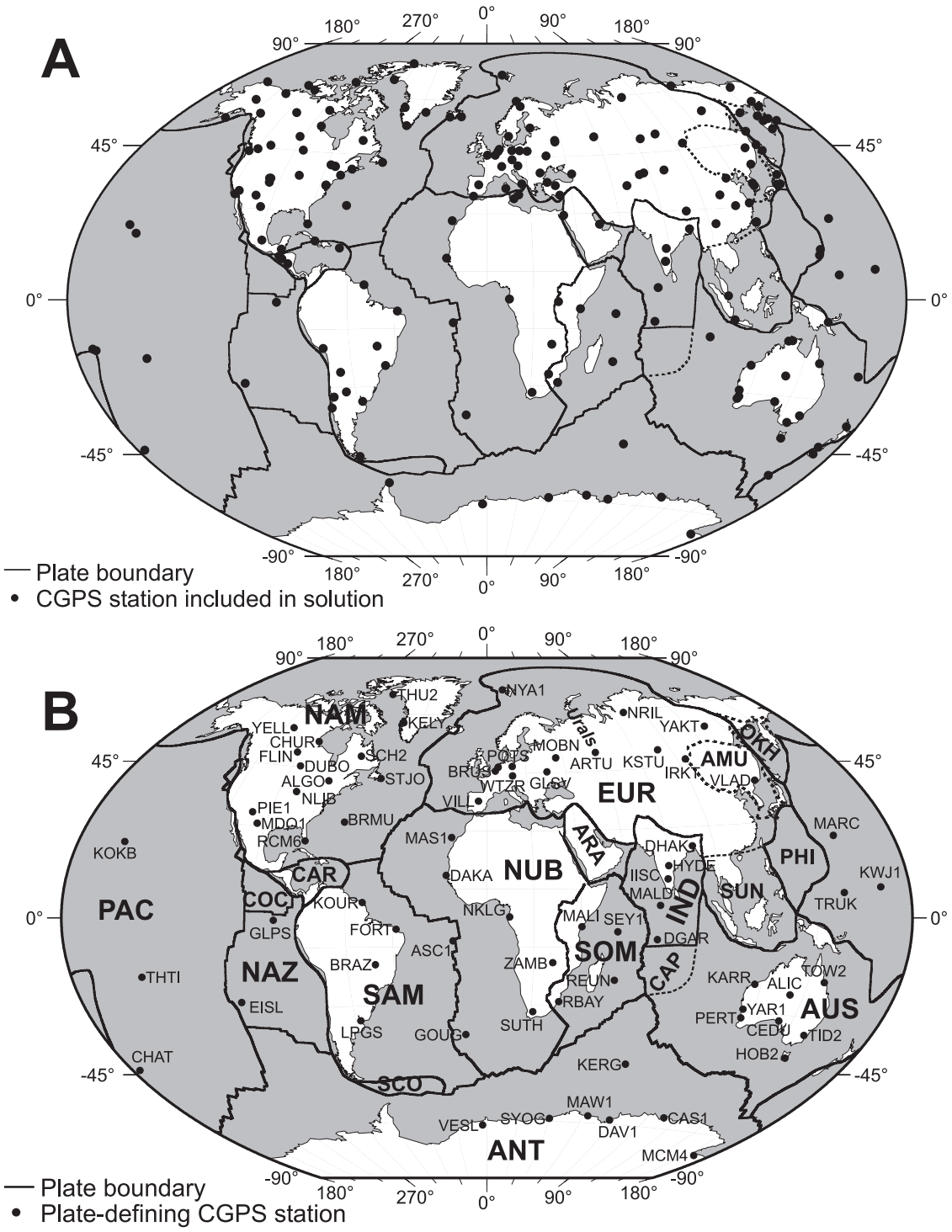

Figure 1. (a) Locations of 192 continuous GPS stations included in the GPS solution in this study. (b) Locations of 71 stations selected to represent the motion of rigid plates. Ten plates labeled in larger letters are analyzed in this study. Continuous lines indicate well-defined plate boundaries; dashes indicate plate boundaries in deforming regions or the boundaries about which there is no agreement among scientists. Full names of analyzed plates are PAC, Pacific; NAM, North American; EUR, Eurasian; SAM, South American; AUS, Australian; ANT, Antarctic; NUB, Nubian; SOM, Somalian; IND, Indian; NAZ, Nazca. Other indicated plates are AMU, Amurian; ARA, Arabian; CAR, Caribbean; OKH, Okhotsk; PHI, Philippine; COC, Cocos; SCO, Scotia; CAP, Capricorn; SUN, Sunda.

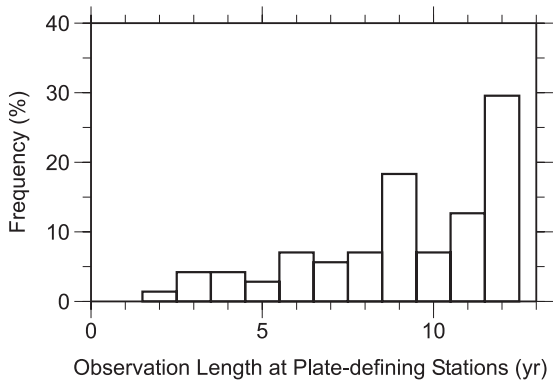

Figure 2. Distribution of lengths of time series for the plate-defining stations selected in this study.

origin is drifting relative to CP. Therefore, we estimate both the plate rotation rates and this drift by minimizing the misfit between horizontal GPS velocities and predictions of the plate model. Horizontal GPS velocities constrain the translation rate of CP because the nonzero rate would make the plates appear deforming (see section 2.2). Mathematically, our definition of CP is equivalent to applying the CL constraint to the misfit between modeled and observed velocities. We treat the rotation rates of plates and the translation rate of CP as unknowns, in contrast to *Heki* [1996], who fixed the rotation rates of plates to the rates of the NUVEL-1A geologic plate model.

[6] The solution for the plate motions presented here is independent of ITRF and allows us to assess translation rates of various ITRF realizations relative to CP. Variants of this approach were used in the following studies: (1) *Argus et al.* [1999], analysis of the global VLBI and SLR solutions; (2) *Steblov et al.* [2003], GPS solution for the motion of three plates: the North American, Eurasian, and Pacific; and (3) *Argus* [2007], evaluation of relative drifts of reference frames associated with different space geodetic techniques.

[7] The model of the plate kinematics presented here addresses the problem debated since the beginning of the space geodesy, How big are disagreements between the current plate motions and the motions averaged over several million years, the "geologic" timescale [*Argus and Heflin*, 1995; *Larson et al.*, 1997; *DeMets and Dixon*, 1999; *Kogan et al.*, 2000; *Beavan et al.*, 2002; *Sella et al.*, 2002; *Calais et al.*, 2003a; *Steblov et al.*, 2003]? Some discrepancies between geodetic and geologic models were resolved due to improvements in the geologic plate model based on updated marine magnetic surveys [*DeMets and Dixon*, 1999; *Calais et al.*, 2003a]. Other discrepancies require reinterpretations of plate geometries in terms of two or more smaller plates and belts of distributed deformation [*Gordon et al.*, 1998; *Bird*, 2003; *Horner-Johnson et al.*, 2007]. Nevertheless, there is evidence that the motion of some plates over the geologic timescale differs from the motion estimated geodetically over a time interval of several years [*Calais et al.*, 2003a; *Steblov et al.*, 2003].

[8] In this paper, the vectors of relative rotation of adjoining plates are evaluated and compared with the published models, both geodetic and geologic. We then discuss the integrity of individual plates as exhibited by plate-residual station velocities.

2. Data and Analysis

[9] Here the multiyear GPS solution is defined as a set of loosely constrained station positions and velocities and their covariance matrix. The matrix is rank deficient with respect to rotation (the same is true for all geodetic methods) and it poorly constrains translations; the latter property is explained by higher accuracy of interstation baselines in comparison with GPS satellite orbits [*Dong et al.*, 1998]. Although the estimated parameters are weakly constrained, their frame-invariant combinations such as interstation baselines and their rates of change are accurately determined and can be mapped into horizontal and vertical station velocities once the center of plate rotation is established.

2.1. Derivation of Loosely Constrained Multiyear Solution

[10] Several publications provide details on how to process GPS phase observations by the GAMIT/GLOBK software with the goal to estimate station positions and velocities [*McClusky et al.*, 2003; *Steblov et al.*, 2003; *Herring*, 2005; *King and Bock*, 2006]. Here we summarize individual steps characterizing our solution, which is based on GPS observations collected at 192 globally distributed stations (Figure 1a and Data Set S1 of the auxiliary material[1]). Of the 71 stations that are assumed to represent rigid plate motion (plate-defining stations), 67 stations were observed for >5 years (Figures 1b and 2). The data sources are the following:

[11] 1. Source A is the permanent network of the International GNSS Service (IGS). Using the GAMIT/GLOBK software, we combined all daily GPS solutions of the Scripps Orbital and Permanent Array Center (SOPAC) from 1995.0 to 2007.0; they are called daily global loose solutions in the following text. Each such solution contains estimates of loosely constrained parameters and their covariance matrix. The parameters include station positions, satellite orbital parameters, and Earth orientation parameters (EOP). Two most recent global GPS solutions based on the IGS network, those of *Sella et al.* [2002] and *Prawirodirdjo and Bock* [2004], encompass observations for the time periods: 1993.0–2001.0 and 1991.0–2003.5, respectively. In comparison with *Sella et al.* [2002], we included the time period 2001–2007; in comparison with *Prawirodirdjo and Bock* [2004], we included the time period 2003–2007. Longer time series for the recent period allowed us to evaluate accurate velocities in Africa and in the Arctic region of North America.

[12] 2. Source B is the non-IGS permanent stations on the Pacific, Indian, and North American plates, important for the improved constraint on plate motions. In several cases, we used IGS stations not analyzed at SOPAC (for example, stations REUN and KHAJ). We processed by GAMIT/GLOBK each site of source B together with five to eight nearest IGS sites, to estimate the same set of parameters and their covariance matrix as in source A. Each such regional solution was then combined by Kalman filter with the

[1] Auxiliary materials are available at ftp://ftp.agu.org/apend/jb/2007jb005353.

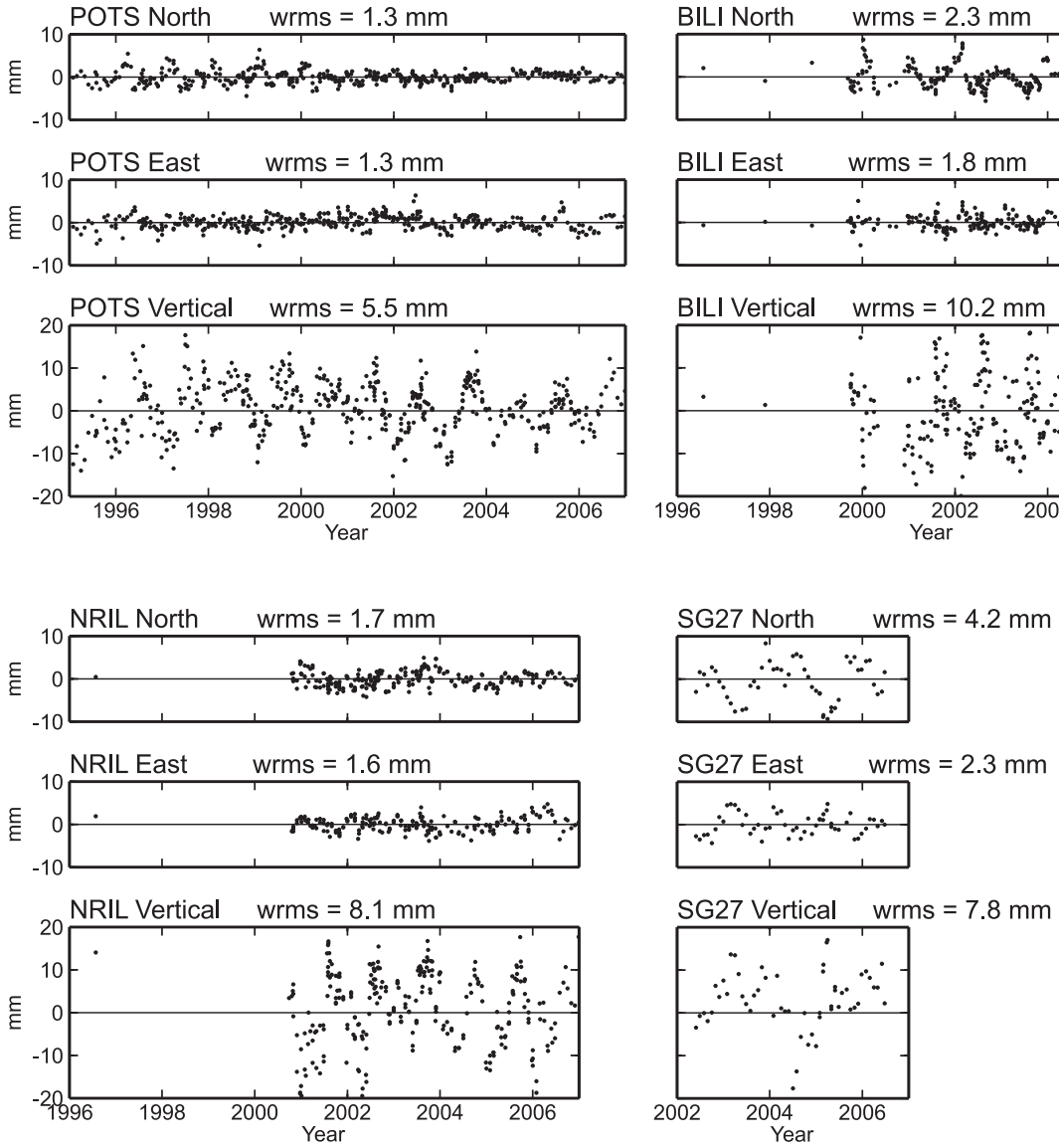

Figure 3. Multiyear GPS time series of stations POTS, BILI, NRIL, and SG27. North, east, and vertical components of positions averaged over monthly intervals are shown with the trend removed. Stations BILI and NRIL were repeatedly observed in survey mode since 1996. Quasiperiodic seasonal variations are conspicuous in vertical components at all stations and in all three components at stations BILI and SG27 in the Arctic region. See Data Set S1 for station locations; wrms, weighted RMS for a component.

global solution for that day, in order to tie the added station to the IGS network.

[13] We use the term "combined daily solution" for a global daily loose solution, estimated from combining sources A and B. The combined daily solution in our processing retains estimates and covariances of station positions only; orbital and EOP information is dropped since it is accurately incorporated in positions due to the global nature of the solution [*Dong et al.*, 1998]. To suppress the noise with periods of several days, the combined solutions were then aggregated by Kalman filter over monthly intervals. Figure 3 illustrates time series of monthly solutions for four stations referenced to ITRF2000. This is not our preferred method of imposing the reference frame for velocities (see section 2.2); however, it is quite adequate for estimating the station noise from the month-to-month repeatability.

[14] At a final step, we combined all monthly solutions by Kalman filter to estimate station positions and velocities and their covariances. The error model for monthly solutions used here is the same as from *Steblov et al.* [2003]; that is, two kinds of noise were superposed: (1) white noise with an amplitude of 2 mm in both horizontal components and 6 mm in the vertical, and (2) time-dependent noise modeled as the random walk with an amplitude of 2 mm/$(a)^{1/2}$ in all three components. The white noise (spectral index 0) reflects fluctuations such as the tropospheric noise, while the random walk implemented in GLOBK (spectral index 2) reflects the monument instability or potential mismodeling of orbits and atmosphere. According to *Mao et al.* [1999], the flicker noise (spectral index 1) is more consistent than the random walk with the time-dependent behavior of GPS time series. The flicker noise, in comparison with the

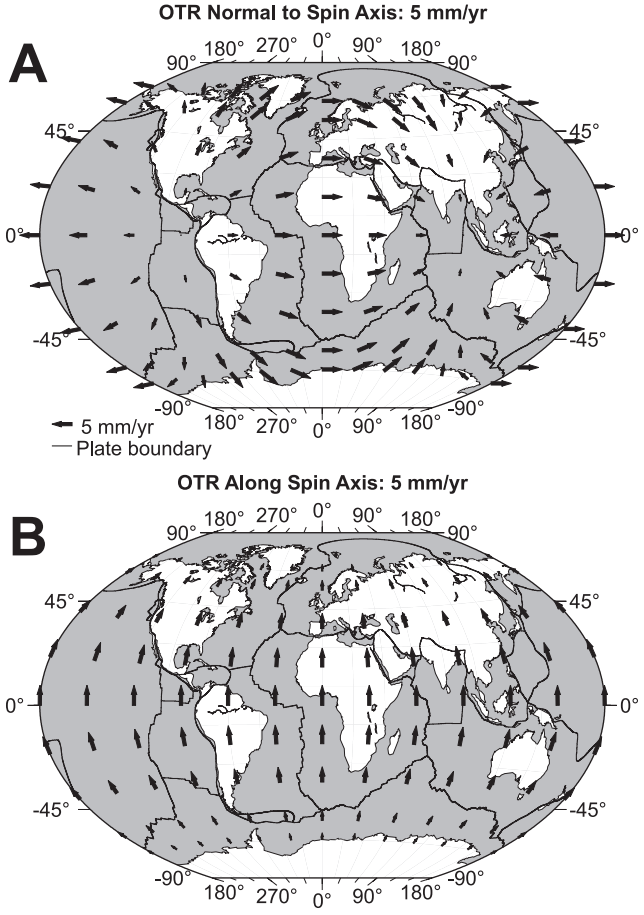

Figure 4. (a) Horizontal velocities at the Earth's surface arising from the origin translation rate (OTR) normal to the Earth's spin axis, set to 5 mm/a. (b) Same as Figure 4a except for OTR parallel to the spin axis.

random walk, yields smaller RMS of estimated parameters; therefore the errors in station positions and velocities in our solution probably are exaggerated.

[15] Discontinuities in station positions caused by coseismic and postseismic displacements were treated in such a way as not to bias interseismic station velocities; more specifically, time- and space-correlated noise was applied to the data after an earthquake, the station was renamed, and the interseismic velocity was estimated from a combination of weighted velocities of original and renamed stations. The capability to model the disruption in time series by imposing the specific stochastic behavior is incorporated in the GLOBK software that we used [*Herring*, 2005]. All such cases are documented in Data Set S1. Positions of all stations in the region of the Indian Ocean were affected by the coseismic and postseismic offsets due to the 2004 Sumatra-Andaman earthquake [*Banerjee et al.*, 2005]. For all stations on the Indian plate except MALD, the velocities before and after the earthquake agree within 2 mm/a.

2.2. Reference Frame Consistent With Plate Kinematics

[16] In this paper, only the kinematic aspect of the reference frame is discussed, i.e., station velocities and their relation to the origin definition.

[17] Estimating plate motions from the GPS solution assumes that the following two points coincide: the reference frame origin (i.e., the origin of the coordinates) and the center of plate rotation CP (i.e., the center of the sphere comprising plates). If, however, these points move relative to each other, then the estimated horizontal and vertical velocities of GPS stations are biased by varying amounts depending on the geographical location (Figure 4) [*Argus et al.*, 1999; *Calais et al.*, 2003a]. In the following, the motion of the reference frame origin relative to CP is called the origin translation rate (OTR). Four methods were proposed to evaluate and suppress OTR:

[18] Method 1 minimizes deviations of the horizontal velocities observed geodetically from those predicted by the geologic plate model NUVEL-1A [*Heki*, 1996]. A problem with this approach is that the current plate motions observed geodetically disagree with NUVEL-1A either because of the nonsteady state motion of plates within the last 3 Ma or because of errors in the geologic model [*Argus et al.*, 1999; *DeMets and Dixon*, 1999; *Calais et al.*, 2003a; *Steblov et al.*, 2003].

[19] Method 2 minimizes vertical velocities of stations observed geodetically [*Argus and Heflin*, 1995; *Argus*, 2007]. Application of this approach to GPS suffers from problems with vertical velocities such as apparent vertical jumps caused by replaced antennas. Typically, vertical GPS velocities are less accurate than horizontal velocities by at least a factor of 3 (Figure 3).

[20] Method 3 places the reference frame origin at the center of plate rotation (CP) estimated from the GPS observations themselves. This result is achieved by estimating plate rotation vectors under no-net translation condition imposed on the plate-residual station velocities [*Argus et al.*, 1999; *Steblov et al.*, 2003; *Argus*, 2007]. We chose such approach in this study.

[21] Method 4 best fits all three station velocity components to the values provided for core stations by a reference frame of the ITRF series [*Altamimi*, 2006].

[22] In the past decade, method 4 was commonly used to fix the origin in GPS solutions. This method suffers from uncertainties in the SLR data used to define the origin in ITRFs.

[23] In section 2.3, we provide details on how the plate kinematics can be derived from the global GPS observations themselves without reference frames imposed a priori, i.e., by method 3. We also estimate how well the origins of ITRF realizations agree with CP.

2.3. Evaluation of Plate Rotations in the Plate-Consistent Reference Frame

[24] It is a common practice to estimate the plate motions from GPS using ITRF reference frames in two steps: (1) best match station positions and velocities from the geodetic solution to a reference frame of the ITRF series; and (2) for each plate j, estimate the rotation vector $\mathbf{\Omega_j}$ by solving a set of observation equations for the horizontal GPS velocities $\mathbf{v_{ij}}$ of stations i on that plate:

$$\mathbf{v}_{ij} + \boldsymbol{\delta}\mathbf{v}_{ij} = \mathbf{\Omega}_j \times \mathbf{r}_{ij}, \tag{1}$$

where $\mathbf{r_{ij}}$ is the geocentric station position vector and $\boldsymbol{\delta}\mathbf{v_{ij}}$ is the discrepancy between an observed GPS velocity and a

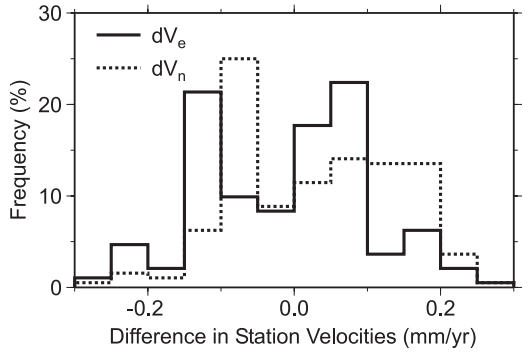

Figure 5. Histogram of differences between GPS station horizontal velocities for two reference frames, both corrected for the origin translation rate: zero-velocity frame and ITRF2005. Differences between east (V_e) and north (V_n) components are plotted. Zero-velocity frame is defined so that a priori station positions do not move with respect to the coordinate system. See *Altamimi* [2006] for definition of ITRF2005.

prediction from the best fitting plate, i.e., the plate-residual station velocity. With this approach, the origin translation rate (OTR) of the reference frame, neglected in equation (1), will bias the estimates of $\mathbf{\Omega_j}$ and $\boldsymbol{\delta}\mathbf{v_{ij}}$. To account for the origin translation rate, equation (1) must be replaced with

$$\mathbf{v}_{ij} + \mathbf{V_T} + \boldsymbol{\delta}\mathbf{v}_{ij} = \mathbf{\Omega}_j \times \mathbf{r}_{ij}, \quad (2)$$

where $\mathbf{V_T}$ is the OTR vector.

[25] In this study, we solved equations (2) by least squares for a set of all plates included in the analysis, using the code available in the GLOBK software. In the following, this solution is called GPS2007.0. Equations (2) can be applied to our loose GPS solution so that ITRF is not required; in this case OTR is estimated for the coordinate system of the loose solution. However, it is useful to apply the ITRF reference frame constraint prior to solving equations (2): it allows us to estimate the drift of ITRF relative to the center of plate rotation CP while it does not affect the estimates of interplate rotation vectors $\mathbf{\Delta\Omega}$ and plate-residual velocities $\mathbf{v_{ij}}$.

[26] To verify that the estimates of $\mathbf{\Delta\Omega}$ and $\boldsymbol{\delta}\mathbf{v_{ij}}$ are independent of a priori reference frames, we tested four frames: ITRF97, ITRF2000, ITRF2005, and the zero-velocity frame. The last frame is defined so that a priori station velocities are set to 0; essentially, imposing such frame implies minimization of the sum of squared horizontal velocities for the stations representing the plates. GPS station velocities of all 192 stations referenced to the tested frames are given in Data Sets S2–S5. As expected, the solution GPS2007.0 is independent of the choice of a reference frame: a specific frame only results in the specific origin translation rate $\mathbf{V_T}$ and specific plate rotation vectors $\mathbf{\Omega_j}$, but the plate-residual station velocities and the relative plate rotation vectors $\mathbf{\Delta\Omega}$ are insensitive to the choice of a frame (Figures 5 and 6a). Regardless of the chosen reference frame, plate-residual velocities are stable within 0.2 mm/a, relative plate rotation rates within 0.0001°/Ma, and pole positions within 0.02° (fractions of the RMS uncertainties). Components and accuracy of $\mathbf{\Delta\Omega}$ for all pairs of adjoining plates are given in Table 1.

[27] An estimate of $\mathbf{V_T}$ is well resolved if GPS stations representing the plates are well distributed over most plates. We tested several subsets of plates for the stability of the estimated $\mathbf{V_T}$. For example, in one of the tests we disregarded stations on the North American, South American, Pacific, and Nazca plates: however, the resultant $\mathbf{V_T}$ agrees with an estimate of $\mathbf{V_T}$ from a full set of plates better than 1 mm/a in X, Y, and Z.

[28] If the origin translation rate (OTR) is ignored, the estimated station velocities are biased by the amounts comparable with the magnitude of OTR; as a result, relative plate rotation vectors are also biased. The effect of OTR on evaluation of plate rotations can be measured by the RMS

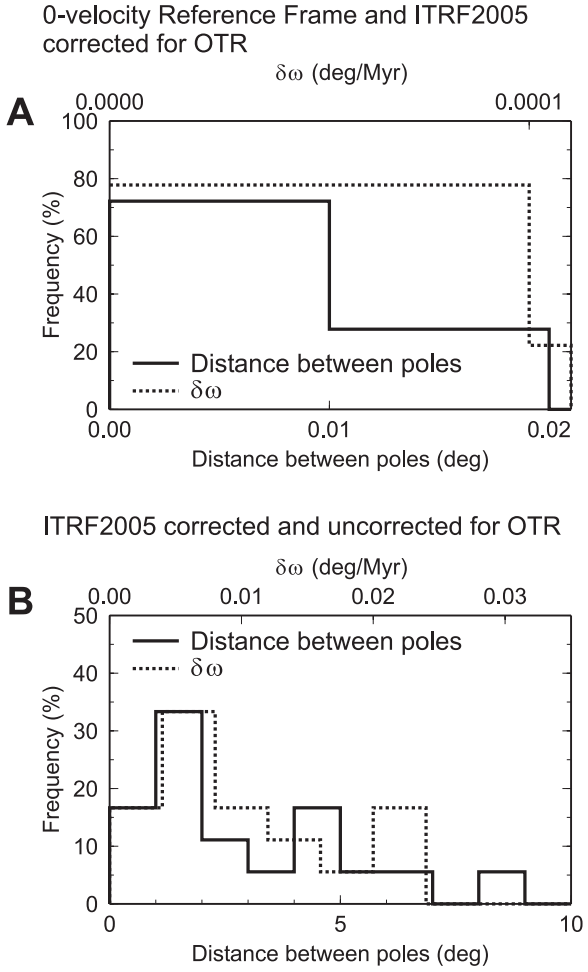

Figure 6. Histograms comparing relative plate rotation vectors for different reference frames. We plot differences in location of poles and rates ($\delta\omega$) of relative plate rotation. (a) Comparison of ITRF2005 and zero-velocity reference frame. Both frames were corrected for the origin translation rate (OTR) estimated from GPS station velocities. The poles and rates of interplate rotation agree better than their standard deviations. (b) Comparison of ITRF2005 with and without correction for OTR. Both poles and rates disagree at a 95% confidence level.

Table 1. Vectors of Relative Rotation for Neighboring Pairs of Ten Plates

Plates Pairs[a]	Vector of Relative Rotation[b]			1σ Error Ellipse[c]			RMS Error of
	Lon, deg	Lat, deg	$d\omega$, deg/Ma	a, deg	b, deg	A, deg	$d\omega$, deg/Ma
ANT-AUS	220.58	−12.77	0.643	0.9	0.5	36	0.003
ANT-NAZ	90.54	−37.79	0.443	2.7	0.8	165	0.014
ANT-NUB	148.03	−5.20	0.116	4.3	2.2	23	0.005
ANT-PAC	275.33	64.92	0.876	0.4	0.3	90	0.008
ANT-SAM	245.55	83.67	0.221	2.0	1.1	110	0.008
ANT-SOM	111.13	−27.48	0.119	6.4	3.3	89	0.009
AUS-EUR	45.02	11.78	0.638	0.8	0.4	121	0.004
AUS-IND	70.61	−14.57	0.288	1.7	1.5	159	0.019
AUS-PAC	4.31	61.28	1.066	0.4	0.3	59	0.007
AUS-SOM	49.16	7.40	0.676	0.8	0.5	130	0.014
EUR-IND	207.11	−27.36	0.441	2.0	0.6	74	0.013
EUR-NAM	137.87	67.41	0.226	1.1	0.8	21	0.004
EUR-NUB	156.41	1.15	0.069	4.1	3.5	165	0.005
EUR-PAC	279.77	63.05	0.903	0.4	0.3	90	0.005
IND-SOM	35.21	20.67	0.452	1.8	1.0	115	0.019
NAM-NUB	272.08	−81.60	0.209	1.6	1.3	84	0.005
NAM-PAC	286.17	51.16	0.766	0.4	0.3	97	0.006
NAM-SAM	308.03	9.19	0.147	2.1	1.3	155	0.008
NAZ-PAC	273.01	55.90	1.285	1.0	0.3	16	0.008
NAZ-SAM	268.96	52.84	0.617	2.1	0.8	9	0.009
NUB-SAM	316.53	62.23	0.260	1.9	1.1	166	0.005
NUB-SOM	32.14	−32.24	0.084	5.2	3.6	29	0.014

[a]The first plate rotates counterclockwise with respect to the second plate around the relative pole. Plate abbreviations are explained in the caption to Figure 1. Zero-velocity reference frame corrected for the origin translation rate (OTR) was used. Regardless of the chosen reference frame, relative plate rotation rates are stable within 0.0001°/Myr, and pole positions are stable within 0.02° (fractions of the RMS uncertainties).
[b]Lon, Lat are longitude and latitude of the relative pole, respectively; $d\omega$ is the rate of relative angular rotation.
[c]The a, b, A are semimajor axis, seminor axis, and azimuth of semimajor axis clockwise from north, respectively.

difference $\|A - B\|$ of rotation vectors for a pair of reference frames A and B:

$$\|A - B\| = \sqrt{\frac{1}{n}\sum_{j=1}^{n} |\mathbf{\Omega_j^A} - \mathbf{\Omega_j^B}|^2}, \quad (3)$$

where $A = (\mathbf{\Omega_1^A}, \ldots \mathbf{\Omega_n^A})$ and $B = (\mathbf{\Omega_1^B}, \ldots \mathbf{\Omega_n^B})$ are the sets of rotation vectors for n plates in reference frames A and B.

[29] Table 2 shows $\|A - B\|$ for several pairs of the following reference frames: ITRF97, ITRF2000, ITRF2005, GPS2007.0 (this study), and geologic plate model NUVEL-1A. The rotation vectors for the ITRF family were estimated by constraining our loose GPS solution with appropriate reference frames without correction for OTR. The agreement among all geodetic solutions is much better than the agreement between any geodetic solution and NUVEL-1A. GPS2007.0 agrees with ITRF2000 and ITRF97 better than with ITRF2005, which clearly reflects that ITRF2005 has the largest OTR.

[30] Because of significant OTR, the vectors of relative plate rotations computed with ITRF2005 differ significantly, depending on whether the OTR correction was estimated or not (Figure 6b). Of all tested reference frames, ITRF2000 is characterized by the smallest OTR of 1.1 mm/a, with all three components less than 1 mm/a (Table 3a). For ITRF97 and ITRF2005, the magnitudes of OTR are 2.1 and 2.6 mm/a, respectively. The large value of OTR in ITRF2005 is caused by Z component in $\mathbf{V_T}$ as large as 2.5 mm/a, well above its RMS uncertainty of 0.2 mm/a. Components of OTR for ITRF2005 agree with components of the drift ITRF2005–ITRF2000 to better than 0.7 mm/a (Table 3a and 3b) [*Dong and Fang*, 2007].

Table 2. Comparison of Plate Rotation Vectors in Different Reference Frames[a]

Compared Pairs of Reference Frames	Correction for the OTR	RMS Difference Between Reference Frames $\|A - B\|$,[b] deg/Ma
A, GPS2007.0[c]	Applied	
B, ITRF97[d]	Not applied	0.012
A, GPS2007.0	Applied	
B, ITRF2000[d]	Not applied	0.010
A, GPS2007.0	Applied	
B, ITRF2005[d]	Not applied	0.024
A, ITRF2000	Not applied	
B, ITRF2005	Not applied	0.017
A, NUVEL-1A	Not applied	
B, GPS2007.0	Applied	0.057
A, NUVEL-1A	Not applied	
B, ITRF97	Not applied	0.061
A, NUVEL-1A	Not applied	
B, ITRF2000	Not applied	0.058
A, NUVEL-1A	Not applied	
B, ITRF2005	Not applied	0.053

[a]The rotation vectors of eight plates (ANT, AUS, EUR, IND, NAM, NAZ, NUB, SAM) are considered with respect to PAC, to ensure the same rotation rate in all reference frames. Plate SOM was disregarded since it is absent from NUVEL-1A.
[b]$\|A - B\| = \sqrt{(1/n)\sum_{j=1}^{n} |\mathbf{\Omega_j^A} - \mathbf{\Omega_j^B}|^2}$, $n = 8$, where $A = (\mathbf{\Omega_1^A}, \ldots \mathbf{\Omega_n^A})$ and $B = (\mathbf{\Omega_1^B}, \ldots \mathbf{\Omega_n^B})$ are the sets of rotation vectors for n plates in reference frames A and B.
[c]The solution derived in this study; see section 2.3 for details.
[d]ITRF97, ITRF2000, and ITRF2005 denote the sets of vectors of plate rotation estimated from our GPS solution with respect to ITRF97, ITRF2000, and ITRF2005. Here corrections for the origin translation rate were not applied.

Table 3a. Origin Translation Rate of ITRF97, ITRF2000, and ITRF2005 Relative to the Center of Plate Rotation: Simultaneous Evaluation of Plate Rotations and OTR From This Study

Reference Frame	OTR			Correlation of Components		
	X, mm/a	Y, mm/a	Z, mm/a	XY	XZ	YZ
ITRF97	−1.6 ± 0.2	−0.2 ± 0.2	−1.3 ± 0.2	0.03	0.12	0.04
ITRF2000	−0.8 ± 0.2	0.4 ± 0.2	0.6 ± 0.2	0.09	−0.02	0.10
ITRF2005	−0.6 ± 0.2	−0.1 ± 0.2	2.5 ± 0.2	0.09	−0.02	0.10

[31] *Argus* [2007] estimated the motion of the center of mass of the whole Earth's system CM in ITRF2000 and ITRF2005 relative to the center of mass of the solid Earth, that is, the CM-CE relative motion. Our estimates of OTR for ITRF2000 and ITRF2005 is the CM-CP relative motion. The CM-CE motion in [*Argus*, 2007] and the CM-CP motion in our study agree within 1 mm/a for each considered version of ITRF. Therefore, the velocity of CP relative to CE is less than 1 mm/a. Discrepancies between our estimates and those of *Argus* [2007] can be attributed to differences in the database: we included observations collected in 2005–2006 and we used a different configuration of stations on several plates.

[32] Since interstation baselines and their first derivatives are the frame-invariant quantities, their accuracy is independent of OTR. For example, OTR is larger for ITRF2005 than for ITRF2000; however, our solution GPS2007.0 agrees with ITRF2005 better than with ITRF2000, after GPS2007.0 is translated and rotated to best fit 37 core stations. The RMS fit to ITRF2005 and to ITRF2000 is 0.2 and 0.4 mm/a per horizontal velocity component, respectively.

2.4. Choice of Plates and of Plate-Defining Stations

[33] In this study, a set of analyzed plates is limited to 10 major plates: Pacific (PAC), North American (NAM), South American (SAM), Eurasian (EUR), Nubian (NUB), Somalian (SOM), Nazca (NAZ), Antarctic (ANT), Australian (AUS), and Indian (IND) (Figure 1b). Several smaller plates shown in Figure 1b were not included for the following reasons: (1) GPS observations do not exist, are limited, or unavailable to us (the Arabian, Philippine, Cocos, Caribbean, Scotia, Capricorn, and Sunda plates); and (2) scientists do not agree whether or not such plates exist (the Okhotsk and Amurian plates).

[34] A total of 71 stations was selected to represent plate motions, starting from the choice as in published studies of the plate kinematics (Table 4 and Figure 1b) [*Dixon et al.*, 1996; *Kogan et al.*, 2000; *Beavan et al.*, 2002; *Sella et al.*, 2002; *Kreemer et al.*, 2003; *Steblov et al.*, 2003; *Prawirodirdjo and Bock*, 2004]. In contrast with our selection, *Argus* [2007] included many more GPS stations in western Europe; we preferred less dense sampling of that region to ensure a proper contribution of Siberian stations to the estimated motion of the Eurasian plate. We selected the stations representing stable plate regions, while rejecting the stations with plate-residual velocities in excess of double RMS uncertainty (Figure 7). Several plate-defining stations are located near plate boundaries (Table 5). Prior to including any such station in the plate definition, the plate rotation vector was estimated without the tested station and the plate-residual velocity of the station was evaluated and inspected for goodness of fit.

[35] In contrast with previous studies, we included in the analysis of plate motions and of plate integrity many stations which previously did not exist, or were observed for a short time interval. The selection of stations on individual plates is explained in more detail below.

2.4.1. North American Plate

[36] A set of plate-defining stations for the North American plate used in this study is the same as from *Steblov et al.* [2003], i.e., avoiding the deforming western United States and Canada [*Freymueller et al.*, 1999; *McCaffrey*, 2005]; however, we also estimated plate-residual velocities of several stations in stable North America, which did not exist by the time of the analysis in *Steblov et al.* Of these new stations, six are in the Arctic region of Canada and in Alaska (SACH, INVK, HOLM, RESO, ALRT, SG27) and one (QAQ1) is in Greenland (Figure 8). We also included in the analysis four continuous stations in east Siberia, which we attribute to the North American plate (BILI, KMS, MAGJ, TIG). The time series of these stations are twice as long in comparison with *Steblov et al.* It is noteworthy that instead of IGS station MAG0, we used its offset continuous station MAGJ because of the long-period instability in the position of MAG0 (Table 6).

2.4.2. Eurasian Plate

[37] In many previous studies, the motion of the Eurasian plate was mostly determined from observations at GPS stations in western Europe. *Steblov et al.* [2003] added observations at stations over Siberia and eastern Europe, a significant improvement in the sampling of the Eurasian plate since Siberia represents three quarters of the plate area. In this study, the time series of observations at Siberian and east European stations are about twice longer than in *Steblov et al.* We note that the winter observations at Siberian station YAKT were disregarded because of the effect of snow accumulation on the antenna.

2.4.3. Pacific Plate

[38] Although we included only six stations to sample the motion of the Pacific plate, they are widely spaced over the plate, were observed for at least 5 years, and have plate-residual velocities less than 1 mm/a. *Beavan et al.* [2002] estimated the motion of PAC using the same continuous stations augmented by six survey mode stations near the

Table 3b. Origin Translation Rate of ITRF2000 and ITRF2005 Relative to the Center of Plate Rotation: Transformation of ITRF2005 to ITRF2000 (ITRF2005 Minus ITRF2000)

Source	OTR			Correlation of Components		
	X, mm/a	Y, mm/a	Z, mm/a	XY	XZ	YZ
IERS[a]	0.2 ± 0.3	−0.1 ± 0.3	1.8 ± 0.3	–	–	–
This study[b]	0.2 ± 0.1	−0.5 ± 0.1	1.9 ± 0.2	–	–	–

[a]Official International Earth Rotation Service 14-parameter transformation based on 70 common stations (data available at http://www.iers.org).

[b]Seven-parameter transformation based on 38 best determined common stations. RMS fit of transformation for horizontal stations velocities is 0.71 mm/a.

Table 4. Plate-Residual Horizontal Velocities of GPS Plate-Defining Stations, Corrected for the Origin Translation Rate[a]

Station	Position[b] Lon, deg	Position[b] Lat, deg	Velocities[c] V_e, mm/a	Velocities[c] V_n, mm/a	1σ Uncertainty[d] σV_e, mm/a	1σ Uncertainty[d] σV_n, mm/a	Correlation V_e, V_n
			Plate ANT				
CAS1	110.52	−66.28	−1.2	0.2	0.6	0.6	0.000
DAV1	77.97	−68.58	0.0	0.2	0.6	0.6	0.000
KERG	70.26	−49.35	0.3	0.3	0.6	0.6	−0.001
MAW1	62.87	−67.61	0.4	−0.6	0.7	0.7	−0.001
MCM4	166.67	−77.84	−0.6	−1.0	0.6	0.6	0.000
SYOG	39.58	−69.01	0.6	−0.7	0.7	0.7	0.000
VESL	357.16	−71.67	0.5	−0.6	0.8	0.8	−0.001
			Plate AUS				
ALIC	133.89	−23.67	0.3	0.3	0.7	0.7	0.000
CEDU	133.81	−31.87	0.7	0.2	0.7	0.7	0.000
HOB2	147.44	−42.80	−0.7	−0.1	0.6	0.6	0.001
KARR	117.10	−20.98	−0.5	0.0	0.7	0.7	0.000
PERT	115.89	−31.80	0.4	0.3	0.6	0.6	0.000
TID2	148.98	−35.40	−0.5	0.3	0.5	0.5	0.000
TOW2	147.06	−19.27	0.1	−0.3	0.7	0.7	0.000
YAR1	115.35	−29.05	−0.5	−0.3	0.6	0.6	0.001
			Plate EUR				
ARTU	58.56	56.43	−0.0	0.6	0.7	0.7	0.000
BRUS	4.36	50.80	0.3	−0.9	0.8	0.8	0.000
GLSV	30.50	50.36	−0.5	0.6	0.7	0.7	0.000
IRKT	104.32	52.22	−0.3	−0.5	0.6	0.6	0.000
KOSG	5.81	52.18	−0.2	0.1	0.7	0.7	0.000
KSTU	92.79	55.99	−0.6	−0.8	0.8	0.8	0.000
MOBN	36.57	55.12	−0.8	1.1	0.9	0.9	0.000
NRIL	88.36	69.36	−0.4	0.4	0.7	0.7	0.000
NYA1	11.87	78.93	−0.8	−0.5	0.5	0.5	0.000
POTS	13.07	52.38	0.0	0.1	0.6	0.6	0.000
VILL	356.05	40.44	0.7	0.1	0.6	0.6	0.000
VLAD	131.93	43.20	0.1	−1.1	0.8	0.8	0.000
WTZR	12.88	49.14	0.3	0.4	0.6	0.6	0.000
YAKT	129.68	62.03	0.4	−0.1	0.7	0.7	0.000
			Plate IND				
DGAR	72.37	−7.27	0.1	−0.5	0.7	0.7	0.000
DHAK	90.40	23.73	0.1	−2.1	1.9	1.8	−0.001
HYDE	78.55	17.42	−1.4	0.5	1.3	1.3	0.002
IISC	77.57	13.02	0.4	0.6	0.7	0.7	0.000
MALD	73.53	4.19	−1.5	2.7	1.8	1.6	0.007
			Plate NAM				
ALGO	281.93	45.96	0.3	−0.7	0.6	0.6	0.000
BRMU	295.30	32.37	0.2	0.1	0.6	0.6	0.000
CHUR	265.91	58.76	1.2	0.2	0.7	0.6	−0.001
DUBO	264.13	50.26	−0.0	0.0	0.7	0.7	0.000
FLIN	258.02	54.73	0.3	−1.1	0.6	0.6	0.000
KELY	309.06	66.99	−0.2	−0.4	0.6	0.6	0.000
MDO1	255.99	30.68	−0.6	0.6	0.6	0.6	0.000
NLIB	268.43	41.77	0.1	0.6	0.6	0.6	0.000
PIE1	251.88	34.30	−0.5	0.1	0.6	0.6	0.000
RCM6	279.62	25.61	2.8	−0.3	1.3	1.2	−0.001
SCH2	293.17	54.83	−0.1	0.5	0.7	0.7	0.000
STJO	307.32	47.59	−0.2	0.5	0.6	0.6	0.000
THU2	291.18	76.54	−0.9	−0.9	0.6	0.6	−0.001
YELL	245.52	62.48	0.5	−0.1	0.6	0.6	0.000
			Plate NAZ				
EISL	250.62	−27.15	0.7	0.3	0.7	0.7	−0.001
GLPS	269.70	−0.74	−1.1	−1.8	1.2	1.2	−0.003
			Plate NUB				
DAKA	342.54	14.69	−0.0	0.4	1.2	1.2	0.000
GOUG	350.12	−40.35	1.3	0.7	0.8	0.8	−0.001
MAS1	344.37	27.76	0.5	−0.7	0.6	0.6	0.000
NKLG	9.67	0.35	−0.5	−0.5	0.8	0.8	0.001
SUTH	20.81	−32.38	−0.6	0.5	0.6	0.6	0.001
ZAMB	28.31	−15.43	−0.2	−0.3	1.1	1.1	0.001
			Plate PAC				
CHAT	183.43	−43.96	0.7	−0.1	0.6	0.6	0.000
KOKB	200.34	22.13	0.6	−0.2	0.8	0.8	−0.001
KWJ1	167.73	8.72	−0.7	0.3	0.9	0.8	0.000
MARC	153.98	24.29	0.5	−0.3	1.1	1.0	−0.003
THTI	210.39	−17.58	−0.5	−0.8	0.8	0.7	0.000
TRUK	151.89	7.45	−1.1	0.8	1.0	0.9	−0.001
			Plate SAM				
ASC1	345.59	−7.95	−0.4	−0.6	0.6	0.6	0.000
BRAZ	312.12	−15.95	0.4	−0.3	0.6	0.6	0.000
FORT	321.57	−3.88	0.1	0.1	0.7	0.7	0.000
KOUR	307.19	5.25	0.1	0.6	0.6	0.6	0.000
LPGS	302.07	−34.91	0.6	−0.6	0.7	0.7	0.001
			Plate SOM				
MALI	40.19	−3.00	−1.6	0.3	0.7	0.7	0.000
RBAY	32.08	−28.80	−1.3	−0.7	0.9	0.9	0.000
REUN	55.57	−21.21	1.5	−0.1	1.4	1.4	−0.004
SEY1	55.48	−4.67	2.2	0.6	0.7	0.6	−0.002

[a]Zero-velocity reference frame corrected for the origin translation rate (OTR) was used. Regardless of the chosen reference frame, plate-residual velocities of the stations are stable to 0.2 mm/a (a fraction of 1σ). ANT, 7 stations, wrms = 0.8 mm/a; AUS, 8 stations, wrms = 0.5 mm/a; EUR, 14 stations, wrms = 0.8 mm/a; IND, 5 stations, wrms = 1.2 mm/a; NAM, 14 stations, wrms = 0.8 mm/a; NAZ, 2 stations, wrms = 1.2 mm/a; NUB, 6 stations, wrms = 0.9 mm/a; PAC, 6 stations, wrms = 0.8 mm/a; SAM, 5 stations, wrms = 0.6 mm/a; SOM, 4 stations, wrms = 1.8 mm/a (wrms is the weighted RMS of the length of velocity vector $(V_e^2 + V_n^2)^{1/2}$).

[b]Geocentric coordinates.

[c]V_e and V_n are velocities to east and to north, respectively.

[d]The parameters σV_e and σV_n are 1σ uncertainties of V_e and V_n, respectively.

boundary of the Pacific and Australian plates in the region of New Zealand.

2.4.4. South American Plate

[39] The strain buildup caused by subduction of the Nazca plate beneath South America is prominent in GPS velocities over the western half of the plate (Figure 7). In this study, the South American plate is represented by four stations on the east coast of the continent and by a station on Ascension Island (ASC1) in the Atlantic Ocean, with plate-residual velocities less than 1 mm/a.

2.4.5. Nazca Plate

[40] The motion of the Nazca plate (NAZ) is estimated from observations at two continuous stations only, the minimal required number. *Kreemer et al.* [2003] combined the velocities at these two sites with survey mode GPS velocities of *Angermann et al.* [1999] at two islands in the eastern part of NAZ. Additional uncertainty in observations on the Nazca plate comes from the fact that the velocities of two stations on the Galápagos Islands: GLPS (current) and GALA (decommissioned) differ by ∼5 mm/a. All published studies use the observations at GALA. Our solution is based on GLPS because it is more recent, observed for 3.5 years, and shows better day-to-day position repeatability.

2.4.6. Nubian and Somalian Plates

[41] In contrast with previous studies, station DAKA (Dakar), observed for 3.5 years, improved the sampling of

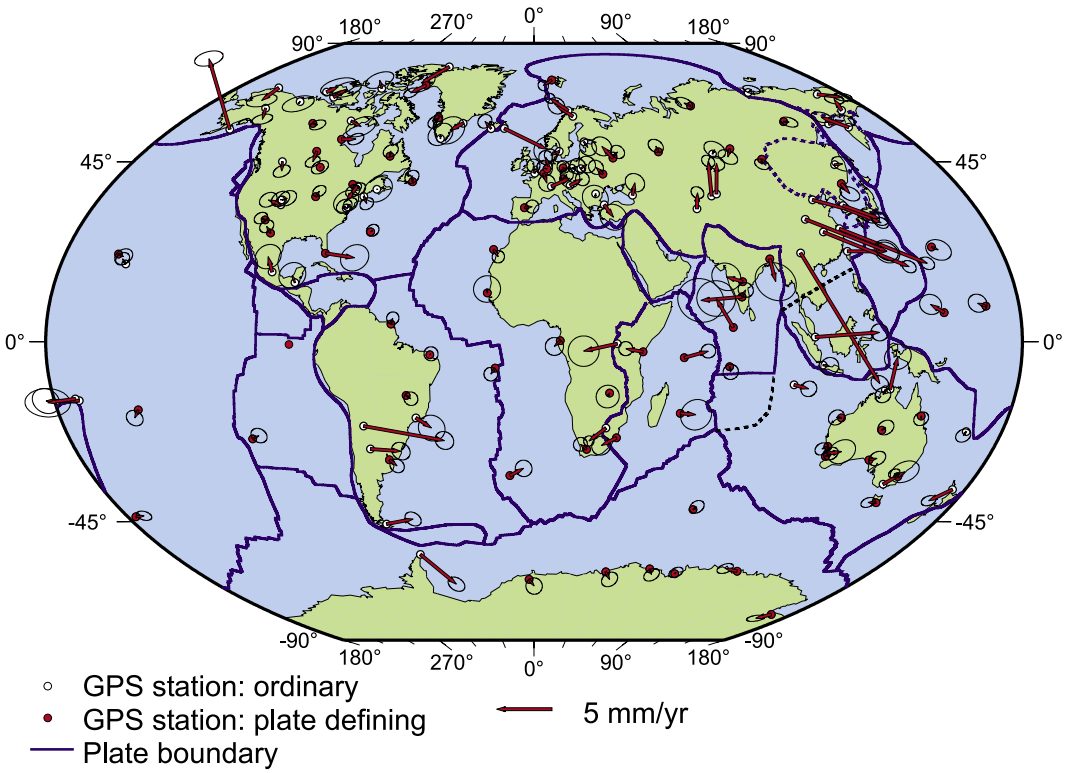

Figure 7. Global plate-residual horizontal velocities of GPS stations estimated in this study, with correction for the origin translation rate applied. Stations with velocity exceeding 20 mm/a are not shown to avoid cluttering. GPS velocities in this figure and in Figures 8 and 9 are shown with 1σ error ellipses.

the Nubian plate (NUB). For the stations sampling the motion of the Somalian plate (SOMA; Figure 1b), we processed about 2 more years of observations (2005–2006) than *Calais et al.* [2006b]. The RMS plate-residual GPS velocity over SOM of 1.8 mm/a is the largest of all other plates (Table 4). Two plate-defining stations in western SOM move westward relative to the plate while two plate-defining stations in eastern SOM move eastward (Figure 7). The problem with estimating the motion of SOM from velocities of existing stations is best understood if the velocities are presented with respect to NUB (Figure 9). Judging from three northern stations, there is a rapid growth in the rate of eastward motion away from NUB with growing distance from the East African rift, the plate boundary. These three stations, MBAR, MALI, and SEY1, are located at similar distances from the pole of rotation NUB-SOM; hence the trend is incompatible with the rigid plate motion. *Fernandes et al.* [2004] and *Calais et al.* [2006b] attribute station MBAR to the East African rift rather than to the Somalian plate. An alternative explanation is that both MBAR and MALI are affected by the distributed deformation associated with the rift. GPS sampling of Somalia could be significantly improved if a station on Madagascar is ever installed.

Table 5. Plate-Residual Horizontal Velocities of GPS Stations Near Plate Boundaries, Corrected for the Origin Translation Rate[a]

			Position		Velocity		1σ Uncertainty	
Station	Plate Defining	Plate	Lon, deg	Lat, deg	V_e, mm/a	V_n, mm/a	σV_e, mm/a	σV_n, mm/a
ASC1[b]	Yes	SAM	345.59	−7.95	−0.4	−0.6	0.6	0.6
ASC1	No	SAM	345.59	−7.95	−0.4	−1.0	0.6	0.6
DGAR[c]	Yes	IND	72.37	−7.27	0.1	−0.6	0.7	0.7
DGAR	Yes	AUS	72.37	−7.27	3.5	−1.6	0.7	0.7
GOUG[b]	Yes	NUB	350.12	−40.35	1.2	0.6	0.7	0.7
GOUG	No	NUB	350.12	−40.35	1.5	0.5	0.7	0.7
NYA1[b]	Yes	EUR	11.87	78.93	−0.8	−0.5	0.5	0.5
NYA1	No	EUR	11.87	78.93	−0.9	−0.7	0.5	0.5
VLAD[b]	Yes	EUR	131.93	43.20	0.1	−1.1	0.8	0.8
VLAD	No	EUR	131.93	43.20	0.2	−1.3	0.8	0.8

[a]See notations to Table 4.
[b]Velocities of ASC1, GOUG, NYA1, and VLAD relative to a plate are presented for two scenarios: (1) the station is included in the estimate of that plate rotation vector (RV); and (2) the station is not included in the estimate of RV.
[c]Velocity of DGAR is presented relative to the Indian (IND) and Australian (AUS) plates.

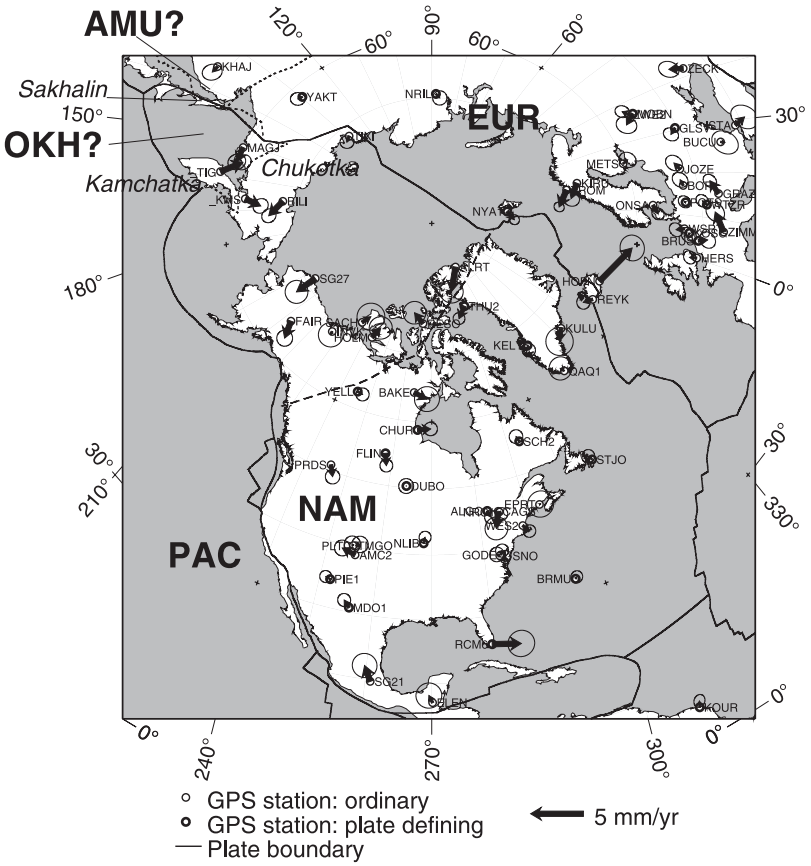

Figure 8. Same as Figure 7 but for the North American plate. The dashed line divides the plate into two parts. The bigger part contains all the stations selected to sample the motion of the North American plate. The smaller part encompasses Arctic Canada, Alaska and northeastern Siberia (Chukotka and Kamchatka). Both parts are tested in this study, whether they make a single North American plate or move with respect to each other.

2.4.7. Australian Plate

[42] The RMS plate-residual GPS velocity over the Australian plate (AUS) is the smallest of all plates analyzed in this study: 0.5 mm/a. To evaluate the motion of AUS, we selected eight stations on the Australian continent and on Tasmania, observed by Geoscience Australia for 9–15 years. It is noteworthy that station COCO in the region of distributed deformation to the northwest of Australia [*DeMets et al.*, 2005] has a small plate-residual speed of 1 mm/a relative to AUS.

2.4.8. Antarctic Plate

[43] The motion of the Antarctic plate (ANT) is exhibited by six stations on the eastern margin of the continent of Antarctica and by a station on Kerguelen Island (KERG). Station OHI3 on Antarctic peninsula is considered anomalous since it is moving southeast at a speed of 3.5 ± 1.0 mm/a relative to the Antarctic plate as defined by all other stations. The anomalous motion of OHI3 can be attributed to the neighborhood of the strike-slip boundary with the Scotia plate. Observations at a semicontinuous GPS station in western Antarctica (1999–2002) confirm the integrity of ANT [*Donnellan and Luyendyk*, 2004].

Table 6. Plate-Residual Horizontal Velocities of Three GPS Stations in the Region of Magadan (East Siberia, Northern Margin of the Sea of Okhotsk), Corrected for the Origin Translation Rate[a]

	Position		Velocities		1σ Uncertainty			
Station	Lon, deg	Lat, deg	V_e, mm/a	V_n, mm/a	σV_e, mm/a	σV_n, mm/a	Correlation V_e, V_n	Interval
MAG0[b]	150.77	59.58	−2.7	−4.1	0.8	0.8	0.000	1997.8–2006.4
MAGJ[c]	150.81	59.58	1.7	0.1	0.8	0.8	0.005	1999.1–2007.0
MAG3[d]	150.68	59.67	2.4	−0.4	1.2	1.2	0.002	1999.8–2004.8

[a]See notations to Table 4.
[b]MAG0 is an official IGS station. Positions of MAG0 show anomalous fluctuations with a period of several years.
[c]MAGJ is an offset continuous station.
[d]MAG3 is an offset survey mode station observed four times in different years for the time period 1998.8–2004.8.

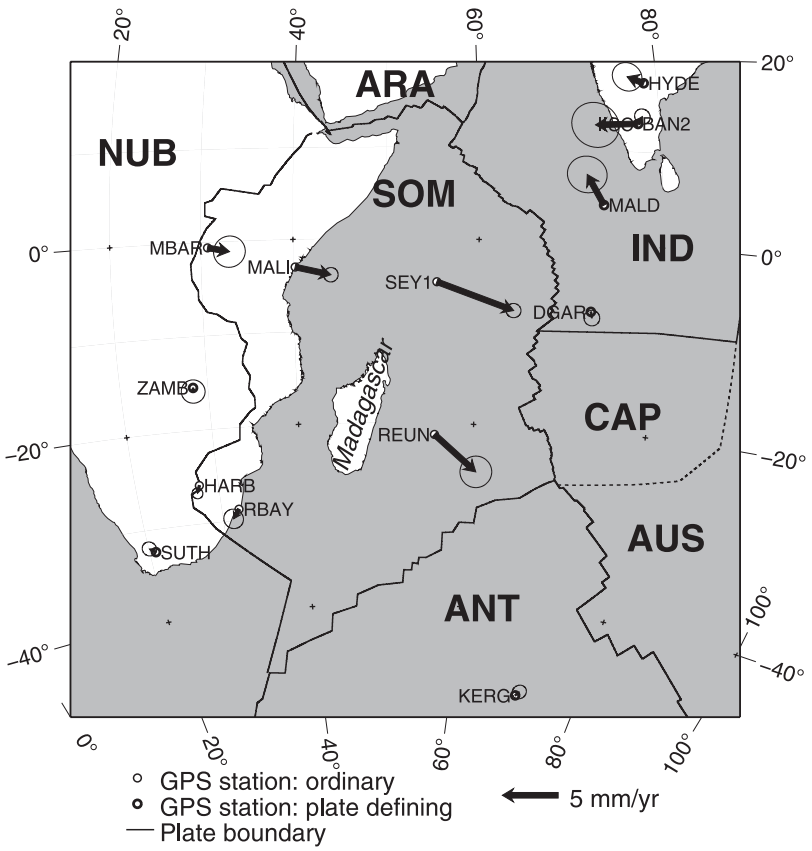

Figure 9. Plate-residual horizontal GPS velocities for the region of the Somalian plate (SOM) estimated in this study, with correction for the origin translation rate applied. In contrast to Figure 7, the velocities over SOM are estimated relative to the Nubian plate.

2.4.9. Indian Plate

[44] A scatter of plate-residual GPS velocities over the Indian plate is about twice larger than on bigger plates (Table 4 and Figure 7). In comparison with previous studies, we added observations of continuous station DHAK in Bangladesh (S. H. Akhter, electronic communication, 15 February 2006). E. V. Apel, R. Bürgmann, and P. Banerjee estimated the motion of the Indian plate by adding several survey mode stations in India and applying corrections for the elastic deformation at plate boundaries (data available at http://seismo.berkeley.edu/annual_reports/ar05_06/node19.html). *Socquet et al.* [2006] included survey mode stations in southern Nepal without corrections for the boundary deformation. Station DGAR at the southern boundary of the Indian plate can be alternatively assigned to the Capricorn or Australian plates, or to the zone of distributed deformation to the south of the Indian plate [*DeMets et al.*, 2005]. We assigned DGAR to the Indian plate because the plate-residual velocity with this assignment is less than 1 mm/a (Table 5). Whether or not DGAR is assigned to IND, the pole and angular velocity of rotation of IND relative to EUR vary insignificantly at a 95% confidence level.

3. Results and Discussion

3.1. Relative Plate Rotation Vectors

[45] Here we compare the plate rotation vectors estimated in our solution GPS2007.0 (Table 1) with previous studies based on GPS and geologic plate models. In general, GPS2007.0 should be more accurate due to larger number of analyzed stations, longer time series, and absence of errors associated with a priori reference frames.

[46] First, we present the statistics of comparisons with the global GPS solutions of *Sella et al.* [2002] and *Prawirodirdjo and Bock* [2004] (Figure 10). The solution of Sella et al. is referenced to ITRF97; the solution of Prawirodirdjo and Bock is referenced to ITRF2000. The poles of GPS2007.0 agree in position with both published solutions within 5° in 75% of cases. The agreement in rotation rates is within 0.05°/Ma in 85%. Deviations of GPS2007.0 from both published solutions exceed 5° in the pole position and 0.05°/Ma in the angular rate if a plate pair contains either the Indian or Nubian plate. For both plates, the database of GPS2007.0 includes observations at several GPS stations established in the last 5 years; therefore, the motion of the Indian and Nubian plates is better determined than in previous studies.

[47] For the second comparison, we chose the following plate pairs that attracted attention of researchers for over a decade: NAM-PAC, NAZ-SAM, NUB-SOM, EUR-NAM, EUR-NUB, and EUR-IND (Figure 11). We compare the rotation vectors of GPS2007.0 with published GPS-based vectors and with geologic vectors updated from the NUVEL-1A [*DeMets et al.*, 1994; *Angermann et al.*, 1999; *DeMets and Dixon*, 1999; *Beavan et al.*, 2002; *Calais et al.*, 2003a; *McClusky et al.*, 2003; *Steblov et al.*, 2003;

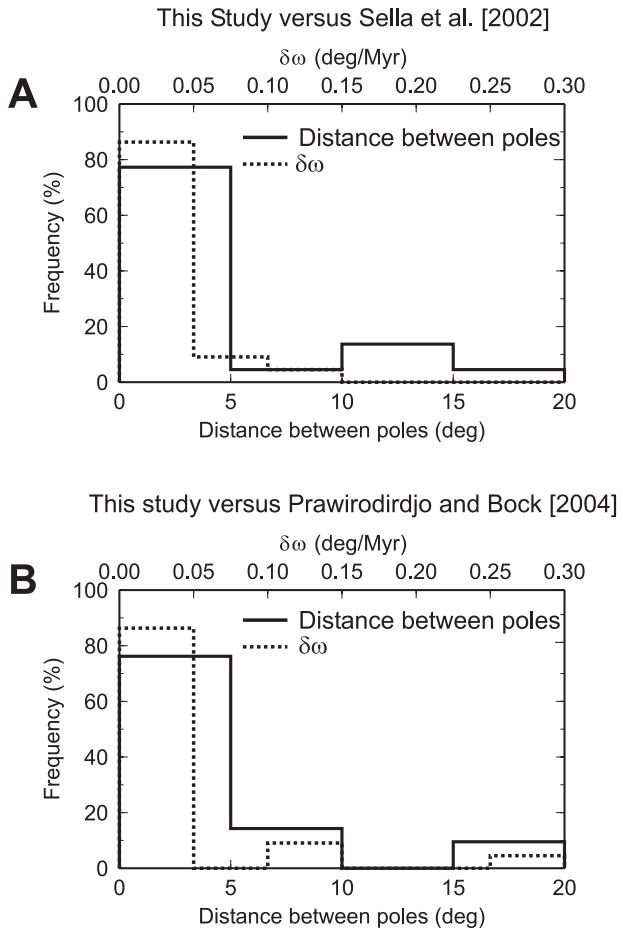

Figure 10. Histograms comparing relative plate rotation vectors estimated in this study with (a) *Sella et al.* [2002] and (b) *Prawirodirdjo and Bock* [2004]. See Figure 6 for explanation of compared quantities.

Prawirodirdjo and Bock, 2004; *McCaffrey*, 2005; *Calais et al.*, 2006b; *Royer et al.*, 2006; *Socquet et al.*, 2006; *Horner-Johnson et al.*, 2007]. For the pairs NAM-PAC, NAZ-SAM, NUB-SOM, and EUR-IND, most GPS estimates of the pole position agree with the geologic pole at a 95% confidence level. For EUR-IND, however, the geologic pole is poorly constrained in the E–W azimuth, so the agreement is not meaningful. For the pairs EUR-NAM and EUR-NUB all poles estimated from GPS differ from the respective geologic poles at a 95% confidence level. In both cases, a geologic pole is offset from a cluster of GPS poles by several hundred kilometers. The smallest scatter of 0.01°/Ma in angular velocities occurs for NAM-PAC. The largest scatter to 0.3°/Ma, both among GPS estimates, and between GPS and geologic estimates, occurs for EUR-IND.

[48] For a given plate, several reasons can cause a deviation of the current (i.e., GPS) rotation vector from the geologic vector representing the average plate motion over the last several million years. The GPS network geometry can be weak; the plates may deform internally; the motion of a plate may accelerate or decelerate within the geologic time interval. We hypothesize that the motion of at least the North American and Pacific plates was stable in the last 3 Ma, judging from the good agreement between well-defined current (GPS) and geologic estimates of the relative pole position and relative rotation rate. If this assumption is correct, then a systematic disagreement between GPS and geologic poles of Eurasia relative to North America implies a nonsteady state motion of the Eurasian plate since 3 Ma.

3.2. North America and Eurasia: Do These Plates Deform?

3.2.1. North American Plate

[49] The question arises, does east Siberia (to the east of the Chersky Range) belong to the North American plate (Figure 8)? Alternatively, the Okhotsk (OKH) and Amurian (AMU) microplates are supposed in place of the North American and Eurasian plates in east Asia [*Zonenshain and Savostin*, 1981; *Seno et al.*, 1996; *Apel et al.*, 2006]. From our solution GPS2007.0, the rotation rate of the Arctic-Siberian part with respect to the main part of the North American plate is statistically insignificant: 0.016 ± 0.011°/Ma; this fact supports the presence of the North American plate in Siberia although the Bering Sea block probably moves with respect to the North American plate [*Fournier and Freymueller*, 2007]. *Prawirodirdjo and Bock* [2004] analyzed the velocities of IGS stations assumed to represent OKH and AMU and found a problem with fitting the velocities by a single rotation vector for each plate.

[50] A test of the plate scenario in east Asia is provided by the detailed GPS survey of Sakhalin Island which is the 800-km-long plate boundary that separates either EUR and NAM, or AMU and OKH, whichever scenario is preferred (Figure 8). From GPS on Sakhalin, the observed convergence rate is 6 mm/a at the north of the island, which is the same rate as predicted by convergence of EUR and NAM (Figure 12). In contrast, the scenario with AMU and OKH predicts much faster convergence at 9 mm/a in northern Sakhalin (overprediction by a factor of 1.5), with increase to 16 mm/a in southern Sakhalin (overprediction by a factor of 3) [*Apel et al.*, 2006; E. V. Apel, electronic communication, 28 May 2007]. Large fault-locking depths are required to reconcile the prediction of AMU and OKH with the observed convergence on Sakhalin; the locking depth of the thrust fault must extend well below the base of the crust to depths of 50–100 km. However, the earthquakes observed on Sakhalin occur at much shallower depths [*Kogan et al.*, 2003]. To summarize, several lines of evidence disagree with the AMU-OKH scenario.

[51] *Calais et al.* [2006c] used 208 continuous GPS stations of the CORS network to the south of ~50°N to estimate the integrity and motion of the North American plate referred to ITRF2000. The stations were chosen to be more than 2100 km away from the center of the glacial isostatic adjustment (GIA) of J. Blewitt et al. (A Stable North American Reference Frame (SNARF): First Release, 2005, available at http://www.unavco.org/research_science/workinggroups_projects/snarf/SNARF1.0/SNARF1.0.html). To compare with Calais et al., we re-ran the GPS2007.0 solution using ITRF2000 without correction for the origin translation rate (Data Set S4); we then compared the resultant rotation vector for NAM with Calais et al. and with other studies (Figure 13) [*Beavan et al.*, 2002; *Márquez-Azúa and DeMets*, 2003; *Prawirodirdjo and Bock*, 2004]. The rotation poles estimated from observations at IGS stations, including our solution, all agree within a spherical distance of ~2°. All

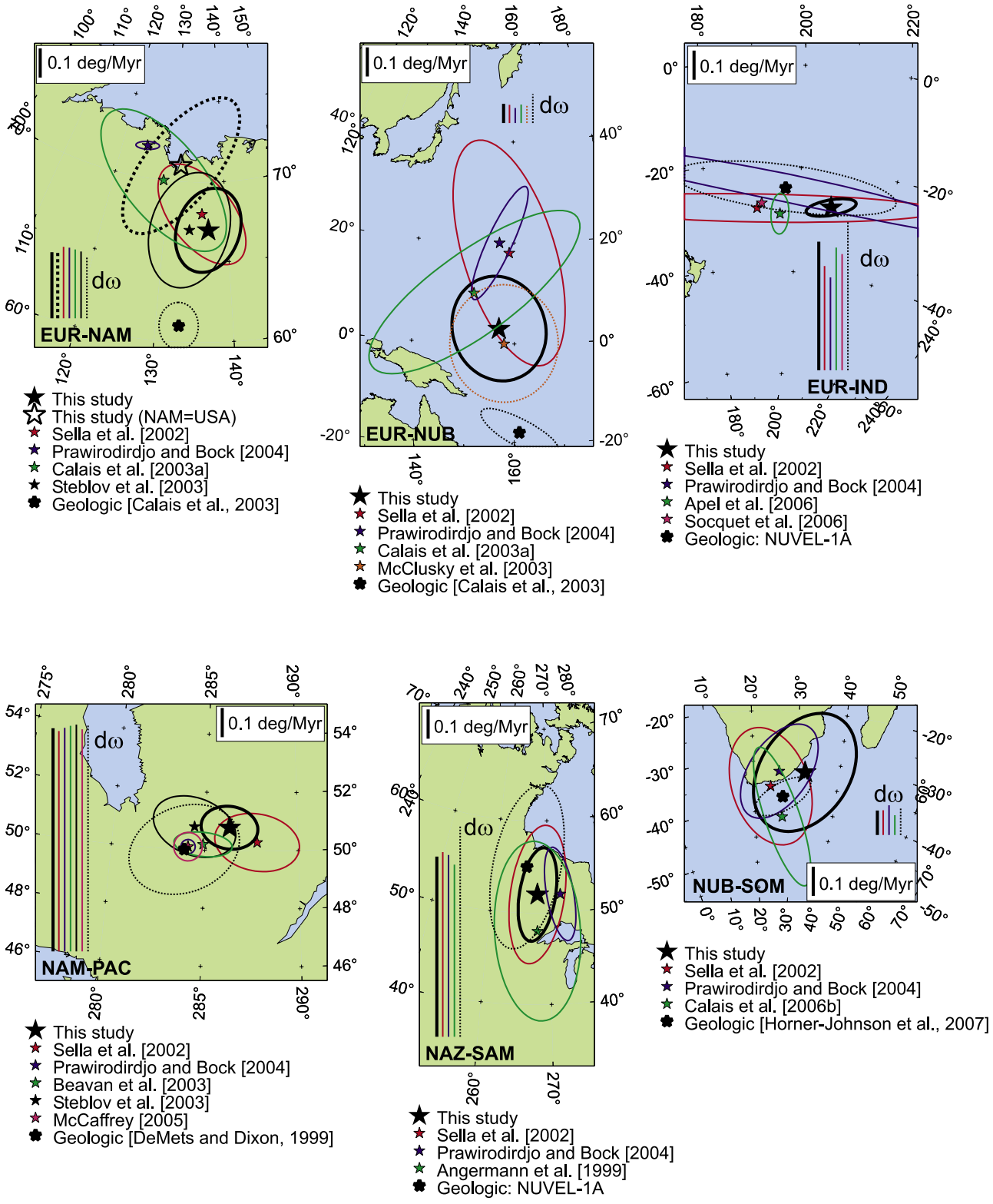

Figure 11. Plots of relative rotation vectors for six plate pairs discussed in literature. We show pole positions with their 95% confidence ellipses and relative rotation rates (vertical bars annotated dω) evaluated in this study and published since 2002. From published geodetic solutions, we selected purely GPS solutions only. Geologic poles and rotation rates are also shown. For the plate pair EUR-NAM (top left plot), our GPS solution is shown in two variants: (1) NAM is defined by 14 stations listed in Table 3, (2) NAM is defined by nine stations far from the region of postglacial rebound (MDO1, PIE1, PLTC, TMGO, NLIB, GODE, USNO, WES2, and BRMU, see Figure 8).

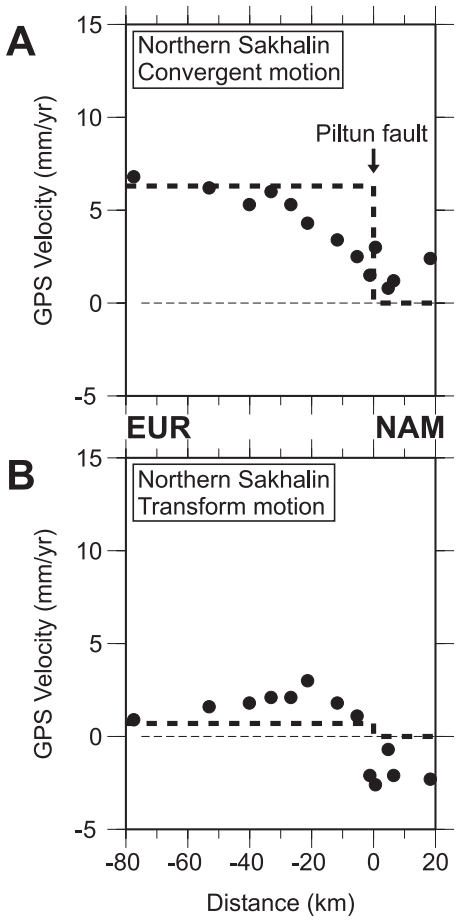

Figure 12. GPS velocities in northern Sakhalin with respect to the North American plate. Observation locations were projected onto a great circle perpendicular to the strike of the Piltun fault thought to be a segment of the plate boundary. (a) Convergent motion (velocity thrust component). (b) Transform motion (velocity right-lateral strike-slip component). Thick dashed line denotes the rate of the relative Eurasian–North American rigid plate motion in the absence of coupling at the fault. Velocities were corrected for the strain buildup caused by subduction of the Pacific plate beneath the Eurasian plate at the Japan-Kuril-Kamchatka megathrust.

these poles, however, lie slightly to the south, by 1–3°, with respect to Calais et al., probably because the effect of GIA was excluded by Calais et al. All estimates of the plate rotation rate agree at a 95% confidence level.

[52] *Sella et al.* [2007] analyzed observations at 362 continuous and survey mode GPS stations in the region around the Hudson Bay and showed that the vertical velocities to 10 mm/a coherently exhibit the uplift and subsidence caused by GIA. However, the horizontal velocities (after removal of the plate rotation) are much smaller, 1–2 mm/a, more scattered and cannot be explained with a single GIA model. We tested whether the relative rotation vector NAM-EUR is affected by inclusion of plate-defining stations in the region of GIA, i.e., in Canada. Two cases were considered: (1) NAM is defined by 14 stations over the whole plate listed in Table 3, (2) NAM is defined by nine stations far from the region of postglacial rebound (MDO1, PIE1, PLTC, TMGO, NLIB, GODE, USNO, WES2, and BRMU). Figure 11 (top left) shows that the pole location and the rotation rate agree at a 95% confidence level in both cases.

3.2.2. Eurasian Plate

[53] Eurasia is the largest plate lying almost completely on the continental landmass. Eurasia is thought to be formed in the Permian by collision of Europe and Siberia, marked by the linear Urals mountain belt trending north-south for 2000 km (Figure 1b) [*Hamilton*, 1970]. We tested whether Europe and Asia continue to move with respect to each other by estimating their relative rotation from two sets of stations, one to the east and the other to the west of the Urals. The rotation rate of 0.02 ± 0.01°/Ma is statistically insignificant, confirming the integrity of the Eurasian plate.

[54] The GPS network used in this study is too sparse to describe the style of deformation in the region of China, a debated subject [*England and Molnar*, 2005; *Calais et al.*, 2006a].

4. Conclusions and Summary

[55] 1. We present the rotation vectors of 10 major plates estimated from GPS observations for the period 1995.0–2007.0. This model of the current plate kinematics should be more precise than earlier models because of the following properties: (1) the database is enhanced in the geo-

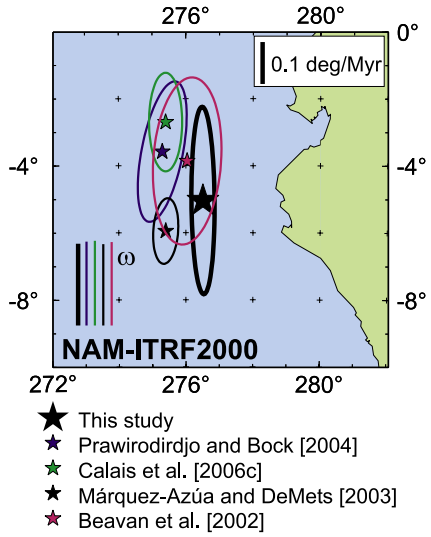

Figure 13. The pole and rotation rate of the North American plate from GPS relative to reference frame ITRF2000 in this study and in literature since 2002. We show pole positions with their 95% confidence ellipses and rotation rates (vertical bars annotated ω). From literature on geodetic solutions, we selected purely GPS solutions only. The pole and rate of *Calais et al.* [2006c] are estimated from several hundred stations to the south of the Hudson Bay, chosen far from the center of the glacial isostatic adjustment (GIA) over the Hudson Bay. All other solutions are based on a much smaller set of stations not necessarily far from the GIA center.

graphical coverage and in length of the time series; and (2) the vectors of plate rotations are independent of ITRF reference frames. The origin of our plate-consistent reference frame is the center of plate rotation (CP) rather than the center of mass of the entire Earth's system (CM) as adopted in recent versions of ITRF. The speed of CP relative to the center of mass of the solid Earth (CE) is less than 1 mm/a.

[56] 2. Our estimate of the speed of the ITRF2005 origin relative to CP is 2.5 mm/a in the Z direction and <1 mm/a in X and Y directions. The drift of the ITRF origin relative to CP cannot be neglected in estimating the plate kinematics.

[57] 3. Although we estimate the rotation vectors of individual plates, only the relative vectors for adjoining plates are discussed; the relative vectors are important since they characterize the strain accumulation at plate boundaries. If needed, our rotation vectors of individual plates can be transformed to satisfy the no-net-rotation condition using the mathematical formalism of *Argus and Gordon* [1991]. Our relative rotation vectors disagree significantly with previous studies for all plate pairs containing either the Indian or Nubian plate. On both plates, we included observations at GPS stations established in the last 5 years; therefore, the motion of India and Nubia is better constrained in this study. Geodetic and geologic vectors of rotation agree well for a pair of the North American plate–Pacific plate; at the same time, the vectors disagree for a pair of the Eurasian plate–North American plate. This result can be interpreted as evidence for the nonsteady state motion of Eurasia since 3 Ma (the time spanned by the geologic model).

[58] 4. The RMS value of plate-residual GPS velocities is 0.5–0.9 mm/a for sets of stations representing the motion of the following plates: Antarctic, Australian, Eurasian, North American, Nubian, Pacific, and South American. This value can be regarded as an upper bound on deviation of real plates from infinite stiffness. The RMS value of plate-residual GPS velocities is 1.2–1.8 mm/a for the Indian, Nazca, and Somalian plates. We attribute higher RMS values for India and Nazca to the noisier data. The higher RMS value for Somalia appears to arise from the distributed deformation to the east of the East African Rift; whether this statement is true can only be decided from observations of denser network in the future.

[59] 5. From the analysis of plate-residual GPS velocities, the Canadian Arctic and northeastern Siberia belong to the North American plate. The detailed GPS survey on Sakhalin Island shows that the Sea of Okhotsk region also belongs to the North American plate. These results provide a constraint on the geometry of the North American plate and put in doubt the existence of smaller plates in northeast Asia.

[60] 6. From the analysis of plate-residual GPS velocities, European and Asian parts of the Eurasian plate do not move relative to each other: that is, the collision of Europe with Asia in the Permian is not inherited in current GPS velocities.

[61] **Acknowledgments.** We thank T. A. Herring and R. W. King for updating the code of the GLOBK software to allow an estimate of the origin translation rate; the Scripps Orbital and Permanent Array Center for public availability of the daily global GPS solutions. We are grateful to D. F. Argus and to the anonymous reviewer for helpful and constructive reviews of this manuscript. Syed Humayun Akhter allowed us to use the observations collected at station DHAK. The GPS survey of Sakhalin was performed in collaboration with N. F. Vasilenko. This work was supported by NSF grants 0408971, 0454894, 0530965, 0630099, 0715360; by JPL grant 1203235; and by IRIS grant 311. All grants were awarded to Lamont-Doherty Earth Observatory of Columbia University. Figures were drawn with the GMT software [*Wessel and Smith*, 1998]. Lamont-Doherty Earth Observatory contribution 7124.

References

Altamimi, Z. (2006), ITRF2005 origin and scale definition, usage and consequences, *Eos Trans. AGU*, *87*(52), Fall Meet. Suppl., Abstract G33C-05.

Altamimi, Z., P. Sillard, and C. Boucher (2002), ITRF2000: A new release of the International Terrestrial Reference Frame for earth science applications, *J. Geophys. Res.*, *107*(B10), 2214, doi:10.1029/2001JB000561.

Altamimi, Z., X. Collilieux, J. Legrand, B. Garayt, and C. Boucher (2007), ITRF2005: A new release of the International Terrestrial Reference Frame based on time series of station positions and Earth orientation parameters, *J. Geophys. Res.*, *112*, B09401, doi:10.1029/2007JB004949.

Angermann, D., J. Klotz, and C. Reigber (1999), Space-geodetic estimation of the Nazca-South America Euler vector, *Earth Planet. Sci. Lett.*, *171*, 329–334, doi:10.1016/S0012-821X(99)00173-9.

Apel, E. V., R. Bürgmann, G. Steblov, N. Vasilenko, R. W. King, and A. Prytkov (2006), Independent active microplate tectonics of northeast Asia from GPS velocities and block modeling, *Geophys. Res. Lett.*, *33*, L11303, doi:10.1029/2006GL026077.

Argus, D. F. (2007), Defining the translational velocity of the reference frame of Earth, *Geophys. J. Int.*, *169*(3), 830–838, doi:10.1111/j.1365-246X.2007.03344.x.

Argus, D. F., and R. G. Gordon (1991), No-net-rotation model of current plate velocities incorporating plate motion model NUVEL-1, *Geophys. Res. Lett.*, *18*(11), 2039–2042, doi:10.1029/91GL01532.

Argus, D. F., and M. Heflin (1995), Plate motion and crustal deformation estimated with geodetic data from the Global Positioning System, *Geophys. Res. Lett.*, *22*(15), 1973–1976, doi:10.1029/95GL02006.

Argus, D. F., W. R. Peltier, and M. M. Watkins (1999), Glacial isostatic adjustment observed using very long baseline interferometry and satellite laser ranging geodesy, *J. Geophys. Res.*, *104*(B12), 29,077–29,093.

Banerjee, P., F. Pollitz, and R. Bürgmann (2005), The size and duration of the Sumatra-Andaman earthquake from far-field static offsets, *Science*, *308*, 1769–1772, doi:10.1126/science.1113746.

Beavan, J., P. Tregoning, M. Bevis, T. Kato, and C. Meertens (2002), Motion and rigidity of the Pacific plate and implications for plate boundary deformation, *J. Geophys. Res.*, *107*(B10), 2261, doi:10.1029/2001JB000282.

Bird, P. (2003), An updated digital model of plate boundaries, *Geochem. Geophys. Geosyst.*, *4*(3), 1027, doi:10.1029/2001GC000252.

Blewitt, J. (2003), Self-consistency in reference frames, *J. Geophys. Res.*, *108*(B2), 2103, doi:10.1029/2002JB002082.

Calais, E., C. DeMets, and J.-M. Nocquet (2003a), Evidence for a post-3.16-Ma change in Nubia-Eurasia-North America plate motions?, *Earth Planet. Sci. Lett.*, *216*, 81–92, doi:10.1016/S0012-821X(03)00482-5.

Calais, E., M. Vergnolle, V. San'kov, A. Lukhnev, A. Miroshnitchenko, S. Amarjargal, and J. Déverchère (2003b), GPS measurements of crustal deformation in the Baikal-Mongolia area (1994–2002): Implications for current kinematics of Asia, *J. Geophys. Res.*, *108*(B10), 2501, doi:10.1029/2002JB002373.

Calais, E., L. Dong, M. Wang, Z. K. Shen, and M. Vergnolle (2006a), Continental deformation in Asia from a combined GPS solution, *Geophys. Res. Lett.*, *33*, L24319, doi:10.1029/2006GL028433.

Calais, E., C. Ebinger, C. Hartnady, and J.-M. Nocquet (2006b), Kinematics of the East African Rift from GPS and earthquake slip vector data, in *The Afar Volcanic Province within the East African Rift System*, edited by G. Yirgu, C. J. Ebinger, and P. K. H. Maguire, *Geol. Soc. Spec. Publ.*, *259*, 9–22.

Calais, E., J. Y. Han, C. DeMets, and J.-M. Nocquet (2006c), Deformation of the North American plate interior from a decade of continuous GPS measurements, *J. Geophys. Res.*, *111*, B06402, doi:10.1029/2005JB004253.

DeMets, C., and T. H. Dixon (1999), New kinematic models for Pacific-North America motion from 3 Ma to present: 1. Evidence for steady motion and biases in the NUVEL-1A model, *Geophys. Res. Lett.*, *26*(13), 1921–1924, doi:10.1029/1999GL900405.

DeMets, C., R. G. Gordon, D. F. Argus, and S. Stein (1994), Effect of recent revisions to the geomagnetic time scale on estimates of current plate motion, *Geophys. Res. Lett.*, *21*(20), 2191–2194, doi:10.1029/94GL02118.

DeMets, C., R. G. Gordon, and J.-Y. Royer (2005), Motion between the Indian, Capricorn and Somalian plates since 20 Ma: Implications for the timing and magnitude of distributed lithospheric deformation in the equa-

torial Indian Ocean, *Geophys. J. Int.*, *161*, 445–468, doi:10.1111/j.1365-246X.2005.02598.x.

Dixon, T. H., A. Mao, and S. Stein (1996), How rigid is the stable interior of the North American plate?, *Geophys. Res. Lett.*, *23*(21), 3035–3038, doi:10.1029/96GL02820.

Dong, D., and P. Fang (2007), ITRF origin: Diagnosis of current realization, paper presented at EGU 2007, Eur. Geophys. Union, Vienna, Austria.

Dong, D., T. A. Herring, and R. W. King (1998), Estimating regional deformation from a combination of space and terrestrial geodetic data, *J. Geod.*, *72*(4), 200–214, doi:10.1007/s001900050161.

Dong, D., T. Yunck, and M. Heflin (2003), Origin of the International Terrestrial Reference Frame, *J. Geophys. Res.*, *108*(B4), 2200, doi:10.1029/2002JB002035.

Donnellan, A., and B. P. Luyendyk (2004), GPS evidence for a coherent Antarctic plate and for postglacial rebound in Marie Byrd Land, *Global Planet. Change*, *42*, 305–311, doi:10.1016/j.gloplacha.2004.02.006.

England, P., and P. Molnar (2005), Late Quaternary to decadal velocity fields in Asia, *J. Geophys. Res.*, *110*, B12401, doi:10.1029/2004JB003541.

Fernandes, R. M. S., B. A. C. Ambrosius, R. Noomen, L. Bastos, L. Combrinck, J. M. Miranda, and W. Spakman (2004), Angular velocities of Nubia and Somalia from continuous GPS data: Implications on present-day relative kinematics, *Earth Planet. Sci. Lett.*, *222*, 197–208, doi:10.1016/j.epsl.2004.02.008.

Fournier, T. J., and J. T. Freymueller (2007), Transition from locked to creeping subduction in the Shumagin region, Alaska, *Geophys. Res. Lett.*, *34*, L06303, doi:10.1029/2006GL029073.

Freymueller, J. T., M. H. Murray, P. Segall, and D. Castillo (1999), Kinematics of the Pacific North America plate boundary zone, northern California, *J. Geophys. Res.*, *104*(B4), 7419–7441, doi:10.1029/1998JB900118.

Gordon, R. G., C. DeMets, and J.-Y. Royer (1998), Evidence for long-term diffuse deformation of the lithosphere of the equatorial Indian Ocean, *Nature*, *395*, 370–374, doi:10.1038/26463.

Hamilton, W. (1970), The Uralides and the motion of the Russian and Siberian platforms, *Geol. Soc. Am. Bull.*, *81*, 2553–2576, doi:10.1130/0016-7606(1970)81[2553:TUATMO]2.0.CO;2.

Heki, K. (1996), Horizontal and vertical crustal movements from three-dimensional very long baseline interferometry kinematic reference frame: Implications for the reversal time scale revision, *J. Geophys. Res.*, *101*(B2), 3187–3198, doi:10.1029/95JB02845.

Herring, T. A. (2005), GLOBK, Global Kalman filter VLBI and GPS Analysis Program, Version 5.11, Mass. Inst. of Technol., Cambridge.

Horner-Johnson, B. C., R. G. Gordon, and D. F. Argus (2007), Plate kinematic evidence for the existence of a distinct plate between the Nubian and Somalian plates along the Southwest Indian Ridge, *J. Geophys. Res.*, *112*, B05418, doi:10.1029/2006JB004519.

King, R. W., and Y. Bock (2006), Documentation for the GAMIT GPS Analysis Software, Rel. 10.21, Mass. Inst. of Technol., Cambridge, Mass.

Kogan, M. G., G. M. Steblov, R. W. King, T. A. Herring, D. I. Frolov, S. G. Egorov, V. Y. Levin, A. Lerner-Lam, and A. Jones (2000), Geodetic constraints on the relative motion and rigidity of Eurasia and North America, *Geophys. Res. Lett.*, *27*(14), 2041–2044, doi:10.1029/2000GL011422.

Kogan, M. G., R. Bürgmann, N. F. Vasilenko, C. H. Scholz, R. W. King, A. I. Ivaschenko, D. I. Frolov, G. M. Steblov, C. U. Kim, and S. G. Egorov (2003), The 2000 Mw 6.8 Uglegorsk earthquake and regional plate boundary deformation of Sakhalin from geodetic data, *Geophys. Res. Lett.*, *30*(3), 1102, doi:10.1029/2002GL016399.

Kreemer, C., W. E. Holt, and A. J. Haines (2003), An integrated global model of present-day plate motions and plate boundary deformations, *Geophys. J. Int.*, *154*, 8–34, doi:10.1046/j.1365-246X.2003.01917.x.

Larson, K. M., J. T. Freymueller, and S. Philipsen (1997), Global plate velocities from the Global Positioning System, *J. Geophys. Res.*, *102*(B5), 9961–9982, doi:10.1029/97JB00514.

Mao, A., C. G. A. Harrison, and T. H. Dixon (1999), Noise in GPS coordinate time series, *J. Geophys. Res.*, *104*(B2), 2797–2816, doi:10.1029/1998JB900033.

Márquez-Azúa, B., and C. DeMets (2003), Crustal velocity field of Mexico from continuous GPS measurements, 1993 to June 2001: Implications for the neotectonics of Mexico, *J. Geophys. Res.*, *108*(B9), 2450, doi:10.1029/2002JB002241.

McCaffrey, R. (2005), Block kinematics of the Pacific-North America plate boundary in the southwestern United States from inversion of GPS, seismological, and geologic data, *J. Geophys. Res.*, *110*, B07401, doi:10.1029/2004JB003307.

McClusky, S., R. Reilinger, S. Mahmoud, D. Ben Sari, and A. Tealeb (2003), GPS constraints on Africa (Nubia) and Arabia plate motions, *Geophys. J. Int.*, *155*, 126–138, doi:10.1046/j.1365-246X.2003.02023.x.

Prawirodirdjo, L., and Y. Bock (2004), Instantaneous global plate motion model from 12 years of continuous GPS observations, *J. Geophys. Res.*, *109*, B08405, doi:10.1029/2003JB002944.

Royer, J.-Y., R. G. Gordon, and B. C. Horner-Johnson (2006), Motion of Nubia relative to Antarctica since 11 Ma: Implications for Nubia-Somalia, Pacific-North America, and India-Eurasia motion, *Geology*, *34*(6), 501–504, doi:10.1130/G22463.1.

Sella, G. F., T. H. Dixon, and A. Mao (2002), REVEL: A model for recent plate velocities from space geodesy, *J. Geophys. Res.*, *107*(B4), 2081, doi:10.1029/2000JB000033.

Sella, G. F., S. Stein, T. H. Dixon, M. Craymer, T. S. James, S. Mazzotti, and R. K. Dokka (2007), Observation of glacial isostatic adjustment in "stable" North America with GPS, *Geophys. Res. Lett.*, *34*, L02306, doi:10.1029/2006GL027081.

Seno, T., T. Sakurai, and S. Stein (1996), Can the Okhotsk plate be discriminated from the North American plate?, *J. Geophys. Res.*, *101*, 11,305–11,315, doi:10.1029/96JB00532.

Socquet, A., C. Vigny, N. Chamot-Rooke, W. Simons, C. Rangin, and B. Ambrosius (2006), India and Sunda plate motion and deformation along their boundary in Myanmar determined by GPS, *J. Geophys. Res.*, *111*, B05406, doi:10.1029/2005JB003877.

Steblov, G. M., M. G. Kogan, R. W. King, C. H. Scholz, R. Bürgmann, and D. I. Frolov (2003), Imprint of the North American plate in Siberia revealed by GPS, *Geophys. Res. Lett.*, *30*(18), 1924, doi:10.1029/2003GL017805.

Wessel, P., and W. H. F. Smith (1998), New, improved version of Generic Mapping Tools released, *Eos Trans. AGU*, *79*, 579, doi:10.1029/98EO00426.

Zonenshain, L. P., and L. A. Savostin (1981), Geodynamics of the Baikal rift zone and plate tectonics of Asia, *Tectonophysics*, *76*, 1–45, doi:10.1016/0040-1951 (81)90251-1.

M. G. Kogan and G. M. Steblov, Lamont-Doherty Earth Observatory of Columbia University, 61 Route 9W, Palisades, NY 10964, USA. (kogan@ldeo.columbia.edu)